A Novel Active Antenna with Self-Mixing and Wideband Varactor-Tuning Capabilities for Communication and Vehicle Identification Applications

Claudio M. Montiel, *Student Member, IEEE*, Lu Fan, *Member, IEEE*, and Kai Chang, *Fellow, IEEE*

Abstract—**A cavity-backed, Gunn-diode-driven, self-mixing active inverted stripline circular patch antenna has been developed. The antenna provides good radiation performance with cross-polarization levels 18 dB below copolarization at boresight. The self-mixing performance shows that the circuit has a 2-dB conversion gain for IF's up to 450 MHz and a single-sideband noise figure of 12 dB at 200 MHz. The self-mixing antenna is also capable to mix signals with its second-harmonic, providing a conversion loss of 3.7 dB. Also, a varactor diode has been incorporated with a inverted stripline circular patch active antenna to allow for electronic tuning. A 13% tuning bandwidth with a power variation of ±1.0 dB was achieved. A simple equivalent circuit has been used to model the active antenna, and the calculated results agree well with the experimental results. The circuit should have many commercial applications in wireless communications, radar, and sensors, but is particularly suitable for use as a transceiver for short communications links or as a microwave identification transceiver.**

I. Introduction

RECENTLY, active antennas [1], [2], and self-mixing oscillators have attracted a lot of attention because they offer savings in size, weight, and cost over conventional designs. These features make them desirable for possible application in microwave communication systems such as local area networks (LAN's), microwave identification systems, and short distance communication systems. Gunn diodes and FET's can operate as a self-mixing oscillators with conversion gains ranging from of 4.1–13 dB and with single sideband noise figures from 11.5 to as low as 3.3 dB [3]–[5]. Although the above-mentioned configurations deliver somewhat better circuit performance, they do so at the cost of increased circuit complexity. Gunn diodes are capable of delivering similar performance with a much simpler bias circuit. In this paper, a Gunn diode self-mixing oscillator was integrated with an inverted stripline antenna to form an active antenna configuration. The circuit consists of an active transmitter antenna and a Gunn diode oscillator used as the transmitter, local oscillator, and self-mixer. This configuration also allows for the addition of a varactor diode into the resonator cavity to provide electronic frequency tuning.

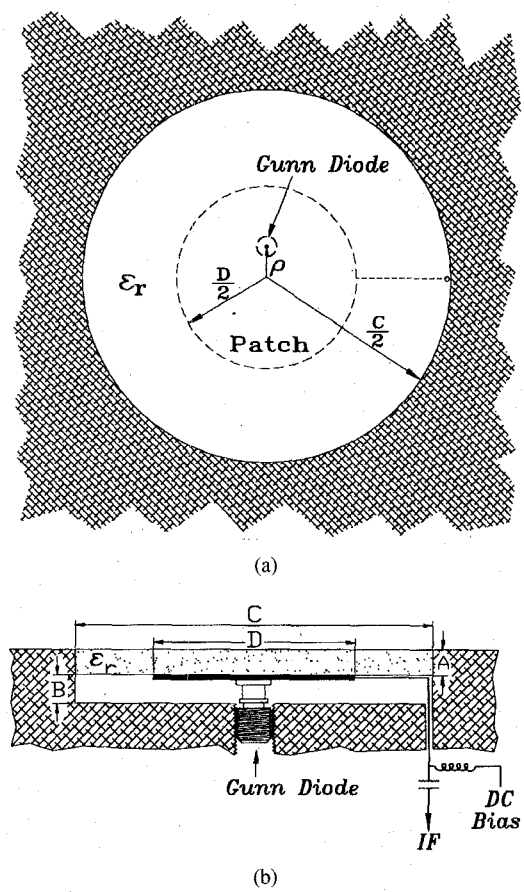

Fig. 1. Configuration of a self-mixing active antenna. (a) Top view showing the Gunn diode placement and (b) side view showing the cavity depth, substrate thickness, dc bias, and IF output.

The active antenna radiates 14.8 ± 1 dBm over a bias tuning range of 200 MHz centered at 6.25 GHz for a bias tuning range of 3.8%. It can be operated as a self-mixing receiver with a conversion gain over 2 dB from 200–450 MHz and a single sideband noise figure of 12 dB at 200 MHz. The antenna also has second-harmonic self-mixing capabilities, but in this case the mixer provides a conversion loss of 3.7 dB. This feature allows the active antenna to be used in identification systems that return a modulated second-

Manuscript received March 27, 1996. This work was supported in part by the U.S. Army Research Office and a U.S. Department of Education Fellowship for Research in Areas of National Need.

The authors are with the Department of Electrical Engineering Texas A&M University, College Station, TX 77843-3128 USA.

Publisher Item Identifier S 0018-9480(96)08517-1.

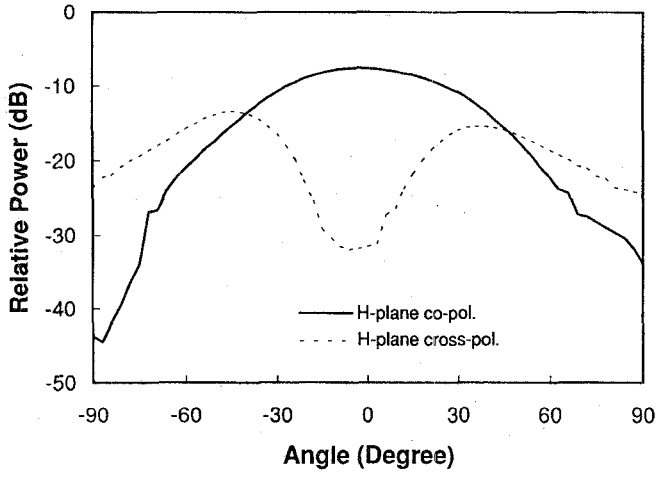

(a)

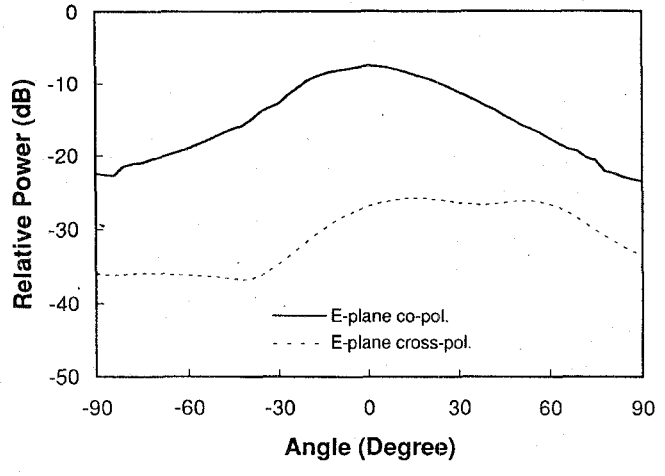

(b)

Fig. 2. Radiation patterns of the self-mixing active antenna. (a) H-plane pattern. (b) E-plane pattern. The solid line represents the copolarization, the dashed line the cross-polarization.

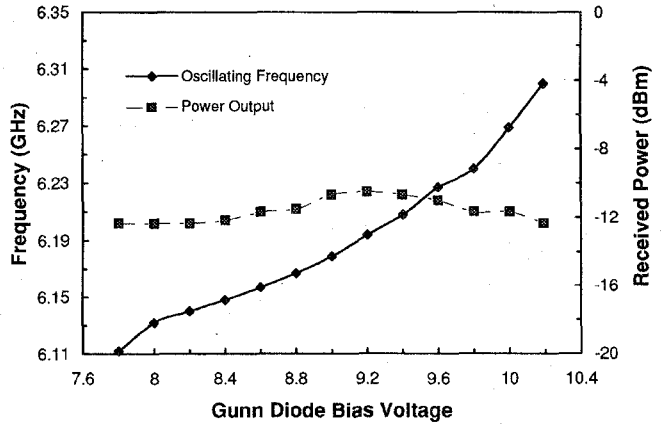

Fig. 3. Active antenna bias tuning performance.

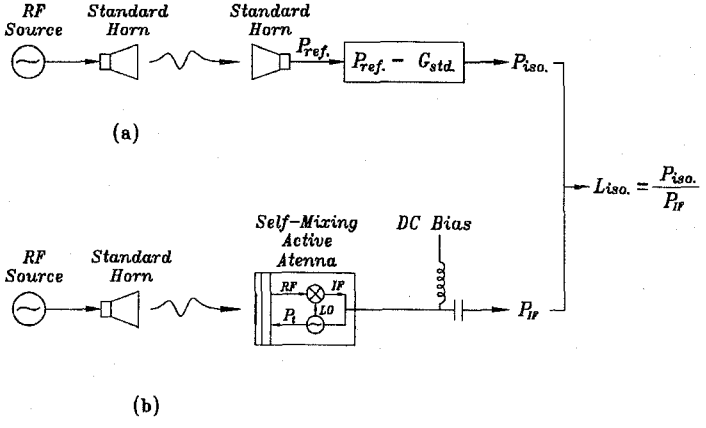

Fig. 4. Test set-up for measuring the conversion gain of the self-mixing active antenna.

harmonic signal, which simplifies transponder design since a microwave source is not needed [6].

Because active microstrip patch antennas generally suffer from having narrow bias tuning ranges and wide output power variations, for some applications varactors have been connected to the radiating elements to minimize these problems [7], [8]. For beam steering power combining arrays, varactor-tuned active antennas with wide tuning ranges can be used to control the phase distribution in the array and to keep minimal power variation over the collective locking range of the active elements. Several other wideband varactor-tuned active antennas have also been developed using varactor tunable notch antennas and tunable power combiners [9] and quasioptical grid VCO's [10]. To further extend the applications for active antennas, spatial power combining, and beam steering, this paper reports a modification of the active inverted patch antenna in [2], by using a varactor-tuned design to realize wideband frequency tuning.

The inverted microstrip patch is attractive for integrated antennas because it offers two distinct advantages. First, diode or probe insertion does not require drilling through the substrate as in microstrip. This characteristic allows for nondestructive device testing and position optimization. Second, the inverted substrate can serve as a built-in radome for protection. By choosing the substrate and metal support carefully, quality hermetic seals can be achieved to protect solid-state devices and improve system reliability and durability.

II. Active Antenna Configuration

Although inverted microstrip has advantages mentioned above, this configuration is prone to exciting surface wave modes which cause considerable cross-talk in dense circuits and high mutual coupling in arrays. Surface modes reduce the antenna radiation efficiency and may distort the antenna pattern. To eliminate unexpected surface modes and reduce coupling, the trapped inverted microstrip is used. The active antenna consists of an inverted stripline circular patch antenna press fitted onto a cylindrical cavity. Fig. 1 shows the circuit configuration of the self-mixing active antenna. The substrate serves as a radome to seal the antenna and circuits. The Gunn diode is offset from the center of the patch by a distance (ρ) of 6 mm, which was determined empirically to provide the best radiation performance. Note that the bias line is perpendicular to the principal polarization for reducing cross-polarization levels. The cavity's depth (B) is 3.0 mm and the patch diameter (D) is 30 mm. The cavity's diameter (C) is 62

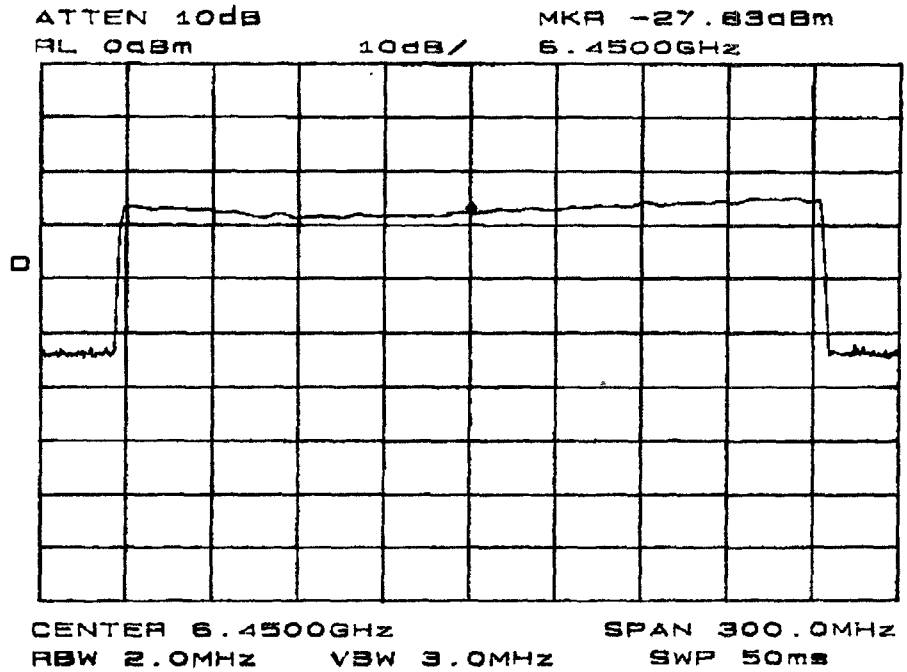

(a)

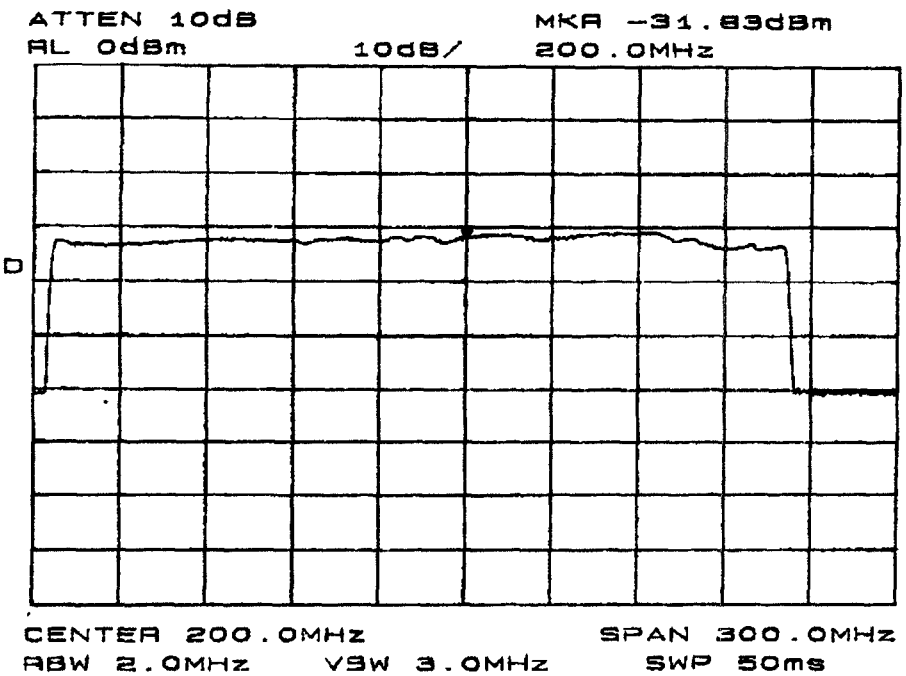

(b)

Fig. 5. Determining the conversion gain at the fundamental frequency. (a) Reference power received and (b) IF power received.

mm and the substrate thickness (A) is 1.524 mm with dielectric constant of 2.3. These dimensions allow the patch to resonate at around 6.3 GHz for probe-fed antennas [11].

Fig. 2 shows the radiation patterns of the self-mixing active antenna. The H-plane and E-plane patterns are smooth with cross-polarization levels of 6 and 18 dB below the copolarization levels. The half-power beamwidths of the H- and E-plane are 57° and 51°, respectively. From the patterns, the equivalent isotropic radiated power (EIRP) and the effective transmitter power (P_{eff}) are calculated using the expressions in [12] and are found to be 431.5 and 30.41 mW. The antenna has a phase noise of −91 dBc/Hz at 100 KHz from the carrier.

The active antenna operates at 6.25 GHz with a bias voltage of 9.4 V and draws 250 mA. The fundamental frequency can, of course, be adjusted to suit the user's needs. The Gunn diode used is a M/A Com, model MA 49135-11. To provide RF, IF, and dc bias isolation, a Hewlett-Packard 11 612B Bias Network was used. The active antenna's tuning range is 200 MHz with radiation power of 14.8 ± 1 dBm for biases from

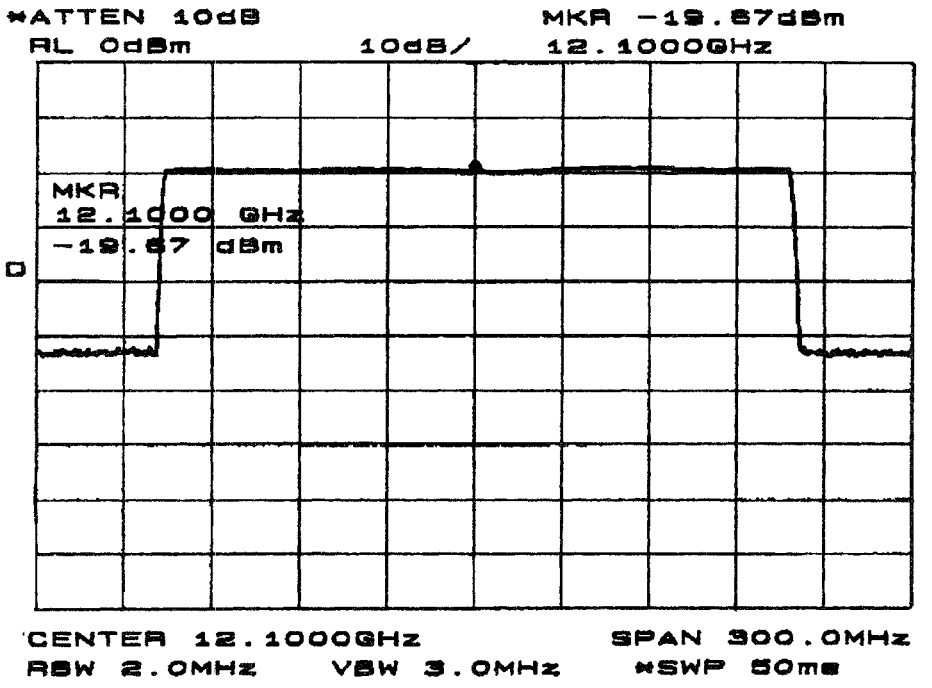

(a)

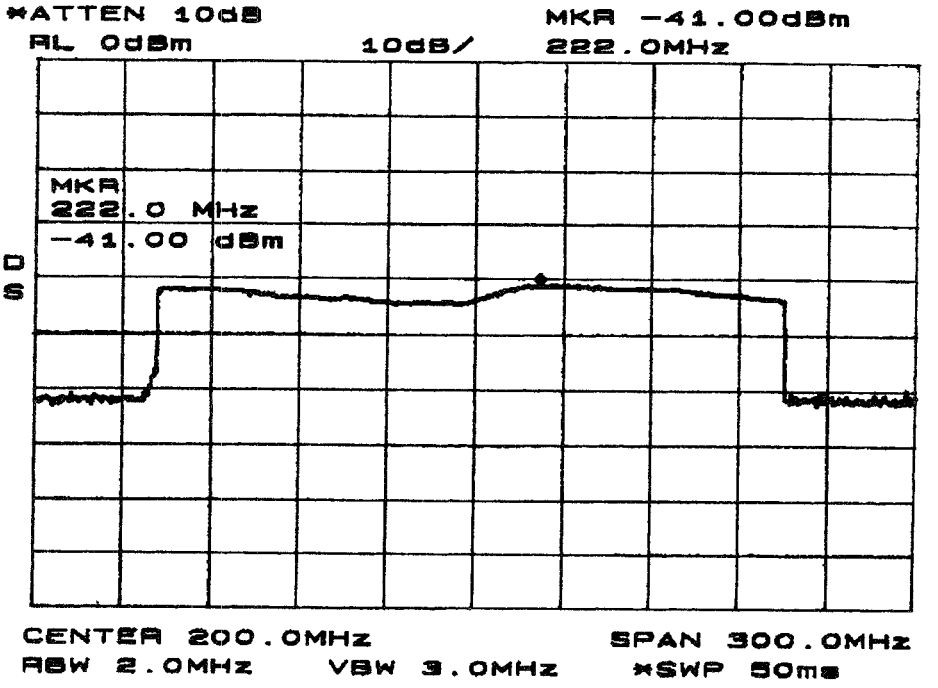

(b)

Fig. 6. Determining the conversion loss at the second harmonic frequency. (a) Reference power received and (b) IF power received.

9–12 V. Fig. 3 shows the bias tuning range and the power output of the active antenna.

III. Active Antenna Performance

A. Conversion Gain and Conversion Loss

To measure the conversion loss (gain) of the self-mixing antenna, a procedure similar to that outlined in [13] was used. Refer to Fig. 4 for the test set-up. The distance separating the transmitting and receiving antennas is 2.0 m. The isotropic conversion loss, in ratio, is defined as

$$L_{iso} = \frac{P_{iso}}{P_{IF}} \tag{1}$$

where P_{IF} is the power delivered at the intermediate frequency and P_{iso} is the power detected at the antenna aperture of the receiving antenna if it were isotropic. Since isotropic antennas are unrealizable, a standard 16-dBi gain horn was used to measure a reference power level (P_{ref}) instead.

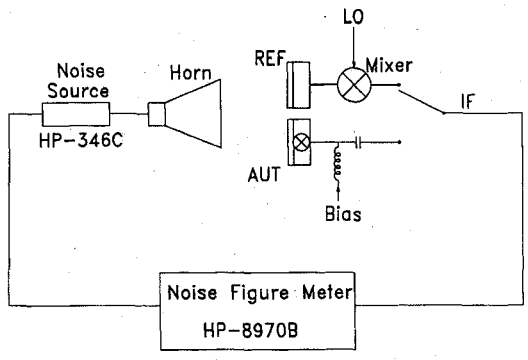

Fig. 7. Noise figure measurement set-up using the HP-8970B noise figure meter.

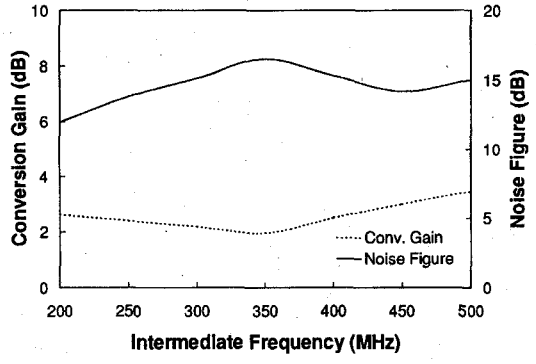

Fig. 8. Conversion gain and noise figure of the self-mixing active antenna.

P_{ref} was measured directly to be -27.83 dBm, as shown in Fig. 5(a). Therefore, we obtain a P_{iso} of -43.83 dBm from: $P_{iso} = P_{ref} - G_{std}$. The IF power of the self-mixing antenna was measured at -31.83 dBm, as shown in Fig. 5(b). The isotropic conversion loss of -12 dB can be obtained from (1). The conversion loss of the self-mixing antenna is: $L_c = L_{iso} + G_{aa}$, where G_{aa} is the gain of the active antenna. In this case G_{aa} is 10 dB, which is consistent with the results reported in [11]. Thus, the conversion loss is -2 dB; i.e., a conversion gain of 2 dB was realized. This is consistent with the results reported in [3]–[5].

Using the same procedure outlined above, the self-mixing performance was measured utilizing the active antenna's second harmonic. In this experiment, the active antenna was biased tuned to oscillate at 6.15 GHz, thus producing a second harmonic frequency of 12.3 GHz. The RF source was then swept for a bandwidth 213.5 MHz centered at 12.1 GHz. This provided an RF–LO separation to center the IF at 200 MHz. Fig. 6(a) and (b) show the measurements of P_{ref} and P_{IF} for the second harmonic at a distance of 85 cm. The resulting conversion loss was determined to be 3.7 dB.

B. Noise Figure

The HP-8970B noise figure meter was used for determining the double sideband noise figure of the self-mixing active antenna. Fig. 7 shows the noise figure measurement set-up. It is important to note that the separation between the standard horn and the other antennas is very short because the noise power delivered by the HP-346C noise source is quite small.

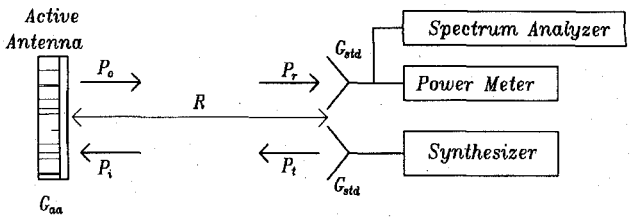

Fig. 9. Test set-up for measuring the injection locking gain and bandwidth.

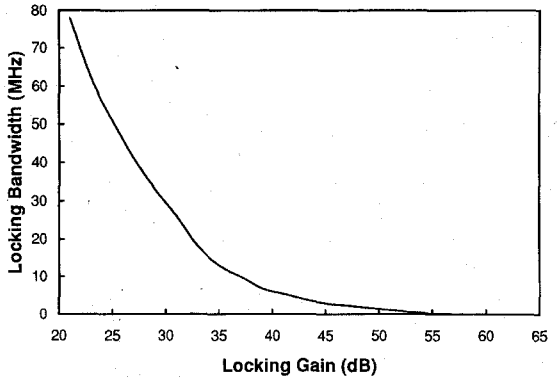

Fig. 10. Active antenna's locking bandwidth versus locking gain.

The measurement procedure is given in the following. A passive probe fed antenna (labeled REF in Fig. 7) of the same dimensions was fitted with an external mixer to provide a noise figure reference. The external mixer was previously characterized with the HP-8970B. Assuming that the differences in noise figure between this reference configuration and the active antenna under test (AUT) are due only to the self-mixing operation, the self-mixing active antenna's noise figure can be obtained from the difference between the reference and the antenna under test, after de-embedding the external mixer data.

Fig. 8 shows the measured conversion gain and noise figure of the self-mixing active antenna after de-embedding reference data. As shown in Fig. 8, the single sideband noise figure varies from 11.97–16.5 dB with a conversion gain greater than 2 dB over an IF bandwidth from 200–500 MHz. The conversion gain results obtained with this method are consistent with those from the test set-up shown in Fig. 4.

C. Injection Locking Bandwidth

Because the active antenna is capable of oscillation over a range of frequencies, it is possible that the input signal injection-lock the oscillator [1], [2] and thus lose the self-mixing action. Although this may be desirable for injection-locked amplifiers, this is undesirable for self-mixing oscillators because it would deprive the self-mixing oscillator of the LO signal.

To determine the injection-locking bandwidth of the self-mixing active antenna, the experimental set-up shown in Fig. 9 was used. Recall that when an external signal at frequency f_i with power P_i is directed at a free-running oscillator operating at frequency f_o with power output P_o, when f_i is close to f_o the free-running oscillator will injection-lock with the external signal and all the output power will be at frequency f_i [14].

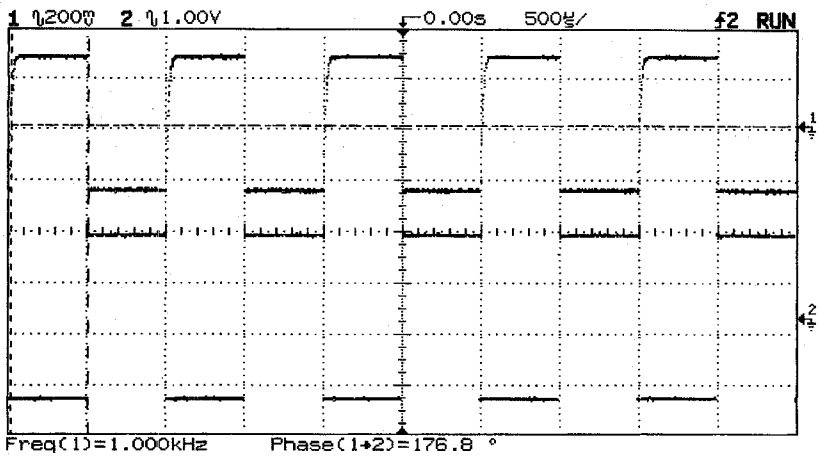

6 GHz carrier pulse modulated with a 1 kHz square wave

Fig. 11. Demodulation performance at the fundamental frequency. Channel 2 (bottom) shows the pulse modulating signal and channel 1 (top) shows the demodulated signal.

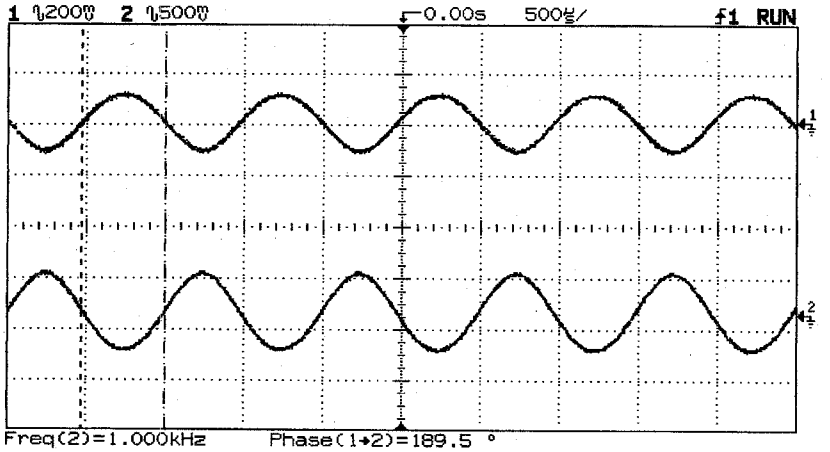

12 GHz carrier amplitude modulated with a 1 kHz sine wave

Fig. 12. Demodulation performance at the second harmonic frequency. Channel 2 (bottom) shows the amplitude modulating signal and channel 1 (top) shows the demodulated signal.

The ratio (P_o/P_i) is the locking gain. The locking range depends on the external Q of the oscillator and the power of the system as given by

$$\frac{2\Delta f}{f_o} = \frac{2}{Q_e}\left(\frac{P_o}{P_i}\right)^{-1/2} \tag{2}$$

where Δf is the one-side locking bandwidth and $2\Delta f$ is the total locking bandwidth, assuming that the upper and lower locking bandwidths are approximately equal, and Q_e is the external Q of the oscillator. It can be shown that Q_e varies from about 60–120 depending on the circuit loading.

Fig. 10 shows the active antenna's total locking bandwidth as a function of the locking gain in dB. The smaller locking bandwidth corresponds to higher locking gain which is equivalent to lower input power. The locking bandwidth is equal to the lowest IF frequency attainable at that input power. Therefore, lower IF's can be attained with lower input power levels. To avoid injection locking in the present device, the input (received) power level must be at least 20 dB below the output (transmitted) power. Thus, the received power must not exceed −5.2 dBm (0.3 mW) or 20 dB below 14.8 dBm.

D. Modulation and Demodulation

Provided that a suitable power supply is available, the active antenna presented here can be modulated using any of the standard techniques such as amplitude, frequency, or pulse modulation. Since the purpose of this experiment was to demonstrate the self mixing characteristics of the Gunn-driven inverted stripline antenna, modulation of this device was not attempted. Instead, the self-mixing receiver's IF output was fed to a coaxial detector. Note that the demodulated signal is 180° out of phase with the modulating signal. The reason for this is that the detector diode used connected in shunt with the coaxial fixture, and introduces a 180° phase shift.

A carrier signal of 6 GHz was pulse modulated with a 1 kHz square wave and transmitted to the self-mixing active antenna. Fig. 11 shows the modulating pulse signal in channel 2 (bottom) and the demodulated signal in channel 1 (top). The

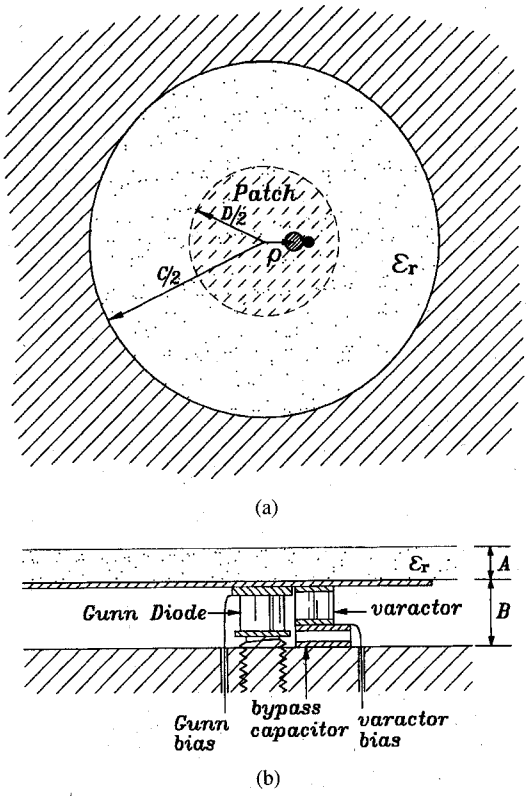

Fig. 13. Configuration of the varactor-tuned active inverted patch antenna. (a) Top view and (b) cross sectional view showing details under the patch.

slight distortion noted was found to come from the detector diode.

To test the self-mixing feature at the second harmonic frequency, a 12 GHz signal was amplitude modulated with a 1 kHz sine wave. Fig. 12 shows the modulating signal in channel 2 (bottom) and the demodulated signal in channel 1 (top).

Detection of frequency modulated signals was also performed with the detector diode using the FM–AM conversion technique. The results, however, were not impressive. Use of a suitable frequency discriminator would yield better results.

IV. Varactor Tuning

Another Gunn-driven active antenna was constructed to investigate the varactor-tuning capabilities of the device. Fig. 13 shows the physical configuration of the varactor-tuned active inverted patch antenna. The antenna includes a circular enclosure which supports the patch insert, chokes out surface waves, and further increases the metal volume for heat dissipation. A screw-type Gunn diode is fastened to a base ground, and a varactor is placed near the Gunn and on top of a bypass capacitor which serves as a dc choke for varactor biasing. A circular patch etched on a circular dielectric insert is pressed into the enclosure over the diodes. The inverted patch serves as a resonant element for the Gunn diode. The optimum position of the diodes within the patch was found experimentally to obtain the maximum operation frequency tuning range with a minimal variation of output power. The diode biases are applied through filtering capacitors below the ground plane.

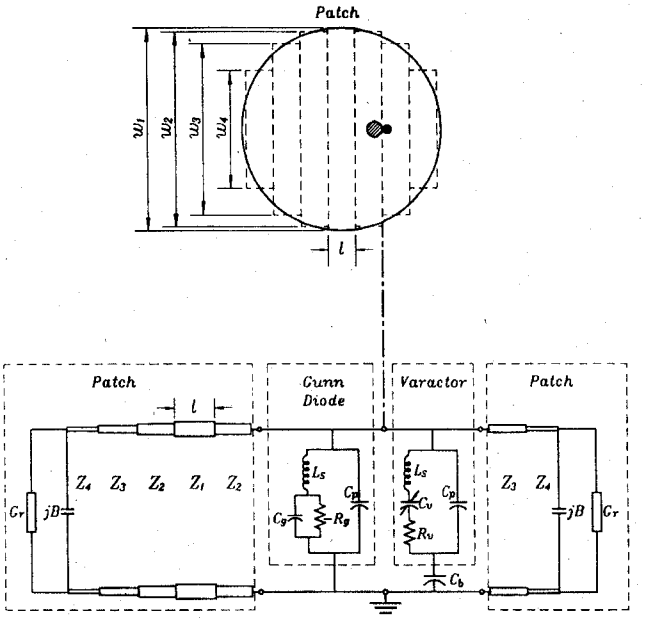

Fig. 14. Equivalent circuit model of the active antenna shown in Fig. 1. Gunn diode parameters: $R_g \approx -8\,\Omega$, $C_g \approx 1.05$ pF, $C_p \approx 0.25$ pF, and $L_s \approx 0.3$ nH. Varactor parameters: $C_v \approx 0.3$–1.0 pF, $C_p \approx 0.05$ pF, $R_v \approx 3\,\Omega$, $L_s \approx 0.3$ nH. Bypass capacitor: $C_b = 100$ pF. G_r is antenna edge admittance and B is the antenna radiating admittance. Both are computed using the equations given in [15].

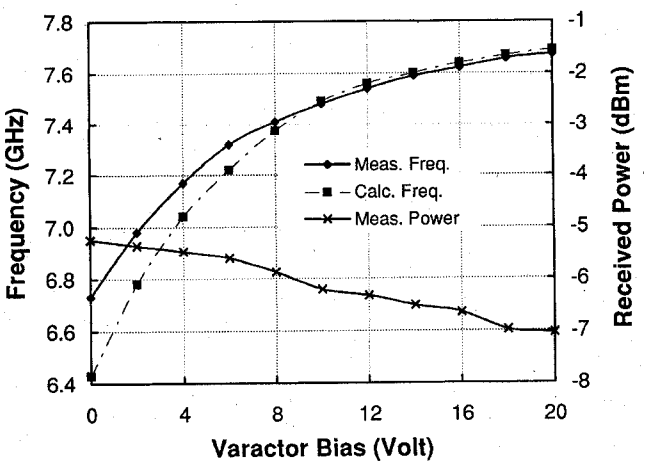

Fig. 15. Measured and simulated frequency and received power versus varactor bias. (Received power is obtained using a Narda 642 standard horn placed 1.1 meters away from the tested active antenna.)

The active antenna was designed at 7 GHz, chosen as the oscillating frequency only for convenient fabrication and test. The varactor-tuned active antenna has the following parameters: substrate thickness A: 1.524 mm, relative dielectric constant ε_r: 2.3, patch diameter D: 24 mm, enclosure diameter C: 62 mm, air spacing B: 3.2 mm, Gunn diode position ρ: 4.5 mm. The Gunn and varactor diodes are M/A COM models MA49135 and MA46601F, respectively. The Gunn produces 16 dBm (40 mW) in an optimized waveguide circuit while the varactor features a maximum to minimum capacitance ratio of about 3.3 (1.0–0.3 pF) over a bias from 0–20 V.

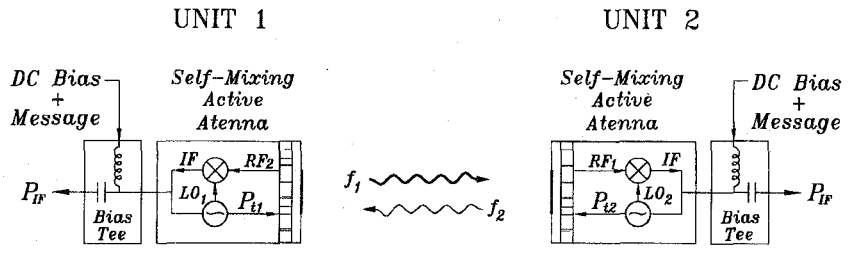

Fig. 16. Proposed communications link using two self-mixing active antennas.

A simple theoretical model was developed to analyze the design. The equivalent circuit can be represented as shown in Fig. 14. The circular patch was approximately modeled by tandem-connected segments of piecewise uniform line of different widths. The edges of the patch are loaded with shunt radiation conductance and fringing capacitances given in [15]. The equivalent circuits of the Gunn and the varactor shown in Fig. 14 were used for simulations. The diode parasitics for the Gunn and varactor are given by the vendor. From circuit oscillating conditions, simulation of the circuit model was performed using Libra [16]. The circular patch was simulated by a cascade of 7 line segments of equal length but different characteristic impedance. The simulation indicated that when the varactor capacitance is varied from 1.0–0.3 pF, the frequency of the antenna should be tuned from 6.4–7.7 GHz as shown in Fig. 15.

The antenna performance was measured in a mini chamber specially made for active antenna testing. The antenna achieved a 13% tuning range of 6.73–7.67 GHz with a power variation of ± 1 dB. As shown in Fig. 15, the calculated tuning curve is in good agreement with the measured tuning results. The differences between the simulations and the measurements are due to the errors in device modeling parameters and the neglecting of the enclosure effects.

The H- and E-plane patterns of the antenna at a representative frequency in the tuning band are essentially the same as those without the varactor, with some minor variations. The half-power beamwidths of the H- and E-plane are 62° and 41°, respectively. The radiation patterns are smooth with cross-polarization levels more than 10 dB lower than the copolarization levels. The H- and E-plane patterns of the antenna at several varactor biases do not show significant variation within the tuning range. It is noted, however, that the radiation power decreases slightly when the varactor bias is increased. The reason for that is an impedance mismatch which gradually increases in the antenna circuit as the varactor bias is changed. From the patterns, the active antenna has an EIRP of 27.3 dBm (537 mW) and a directivity of 12.1 dB, from which a radiated power of 15.2 dBm (33.1 mW) is estimated using the Friis transmission equation. The antenna's phase noise of −85 dBc/Hz at 100 kHz from the carrier was measured using an HP-8562A spectrum analyzer. This specification is 6–9 dB worse than the same active antennas without varactors. A bias tuning bandwidth of 270 MHz centered at 6.85 GHz was observed by varying the Gunn bias from 10–15 V. This tuning range is about 3.9%, which is much smaller compared to the varactor tuning range.

V. Applications

Several applications are possible with the developed self-mixing antenna, depending on whether the designer intends to use the self-mixing character of the device or not. The device can be used as a half-duplex transceiver for short communications links or as a microwave identification system.

A. Half-Duplex Communication System

The oscillation frequency of the active antenna can be modulated by applying a small ac signal to the bias voltage. This allows the oscillator to be frequency-modulated and be used as a transceiver. Fig. 16 shows the communication system set up. It is important to note that, because the RF signal transmitted is also used as the LO reference, simultaneous transmission and reception cannot take place. This makes the self-mixing active antenna suitable for short distance TV transceivers or LAN gateways [15].

The minimum detectable signal can be computed from [14]

$$\text{MDS} = -111 \text{ dBm} + 10 \log \text{ BW} + \text{F} \qquad (3)$$

where BW is the IF bandwidth in MHz and F (dB) is the noise figure of the transceiver. The single sideband noise figure of the transceiver was measured to be 11.97 dB for an IF of 200 MHz.

The MDS is computed to be −91.25 dBm for a typical video bandwidth of 6 MHz. This result, and the Friis transmission equation, can be used to compute the maximum length of a communications link using two of the circuits. For a carrier frequency f_o of 6.25 GHz, the wavelength in free space is 48 mm. The maximum length of the communications link, assuming polarization match and boresight alignment, is computed to be 7.6 km.

The circuit could be frequency modulated by varying the bias voltage to the Gunn diode. The circuit can also be pulse code modulated, provided that a suitable high-current source is used. The data transmission rate would then be determined by the acceptable error rate and switching mechanism chosen.

B. Microwave Identification System

Since the active antenna always transmits a signal, the device can also serve as a self-mixing interrogator for a microwave identification (MW–ID) system. In this case, the

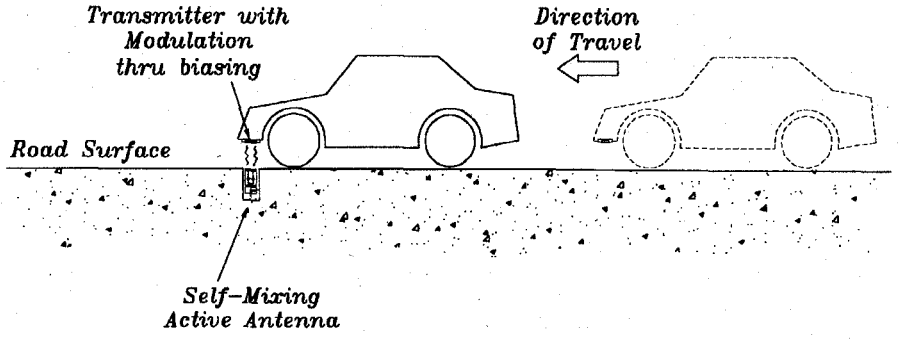

Fig. 17. Conceptual drawing for automated toll collection applications.

free-running oscillator frequency serves as an interrogator beacon and the self-mixing action would down-convert the reply signal which could be pulse code modulated (PCM) with an identification code. Such a system would be suitable for automated toll collection or personnel identification purposes.

An automated toll collection system can be implemented with the self-mixing active antenna presented here. The substrate of the active antenna is press fitted onto the Gunn diode mounting fixture. This assembly in turn can be embedded directly into the road surface in the center of the lane to interrogate oncoming vehicles. The antenna can be aimed toward zenith or tilted slightly toward oncoming traffic, as shown in Fig. 17.

The free-running frequency interrogates the oncoming vehicle. The vehicle's low-power transmitter responds, with its antenna aimed at the ground, at a different frequency to produce an IF in the 200 MHz range. The vehicle's transmitter can be pulse code modulated (PCM) to send an account or vehicle identification number for billing purposes. A similar scheme can be used to restrict vehicular or personnel access to governmental or industrial complexes, but with the self-mixing antenna mounted on a wall or gate to cover a wider area. A transponder card, such as that presented in [6], could then provide the required access code and the active antenna presented here could be used as the interrogator and receiver.

VI. Conclusion

A self-mixing active antenna has been designed and demonstrated. The beauty of the circuit configuration lies in its simplicity: only one device is needed to build a self-mixing oscillator and no complicated biasing schemes are necessary. The circuit radiates a clean spectrum and operates well in self-mixing mode with a conversion gain of 2 dB. Although the cross-polarization levels along the H-plane need to be improved, the circuit has fairly good radiation patterns. The circuit provides a conversion gain of 2 dB when the incoming RF signal is mixed with the fundamental frequency, and a 3.7 dB conversion loss when the incoming RF signal is mixed with the second-harmonic of the active antenna. Also, a 13% electronic tuning range was achieved with a fairly constant output power by using a varactor integrated in the active Gunn diode inverted patch antenna. The wide electronic tuning range is very useful for transmitter, power combining, and active array beam steering applications.

The inverted microstrip circuit offers a compact, simple, low-cost, reproducible, and hermetically sealed source. Because of its good circuit configuration and radiation performance, this tunable active antenna is well suited for commercial and military applications as a transceiver for microwave ID applications or for short communication links.

References

[1] K. Chang, K. A. Hummer, and J. L Klein, "Experiments on injection locking of active antenna elements for active phase arrays and spatial power combiners," *IEEE Trans. Microwave Theory Tech.*, vol. 37, no. 7, pp. 1078–1084, July 1989.

[2] J. A. Navarro, L. Fan, and K. Chang, "Active inverted stripline circular patch antennas for spatial power combining," *IEEE Trans. Microwave Theory Tech.*, vol. 41, no. 10, pp. 1856–1863, Oct. 1993.

[3] G. Milington, R. E. Miles, R. D. Pollard, D. P. Steenson, and J. M. Chamberlain, "A resonant tunnelling diode self-oscillating mixer with conversion gain," *IEEE Microwave Guided Wave Lett.*, vol. 1, no. 11, pp. 320–321, Nov. 1991.

[4] V. D. Hwang and T. Itoh, "Quasioptical HEMT and MESFET self-oscillating mixers," *IEEE Trans. Microwave Theory Tech.*, vol. 36, no. 12, pp. 1701–1705, Dec. 1988.

[5] G. W. Wang, T. Lin, W. Liu, and S. Yang, "A low cost DBS low noise block downconverter with a DR stabilized MESFET self-oscillating mixer," in *IEEE MTT-S Int. Microwave Symp. Dig.*, 1994, vol. 3, pp. 1447–1450.

[6] C. W. Pobanz and T. Itoh, "A microwave noncontact identification transponder using subharmonic interrogation," *IEEE Trans. Microwave Theory Tech.*, vol. 43, no. 7, pp. 1673–1679, July 1995.

[7] P. M. Haskings, P. S. Hall, and J. S. Dahele, "Active patch antenna element with diode tuning," *Elecron. Lett.*, vol. 27, no. 20, pp. 1846–1847, Sept. 1991.

[8] P. Liao and R. A. York, "A varactor-tuned patch oscillator for active arrays," *IEEE Microwave Guided Wave Lett.*, vol. 4, no. 10, pp. 335–337, Oct. 1994.

[9] J. A. Navarro, Y. Shu, and K. Chang, "Broadband electronically tunable planar active radiating elements and spatial power combiners using notch antennas," *IEEE Trans. Microwave Theory Tech.*, vol. 40, no. 2, pp. 323–328, Feb. 1992.

[10] T. Mader, S. Bundy, and Z. B. Popovic, "Quasioptical VCO's," *IEEE Trans. Microwave Theory Tech.*, vol. 41, no. 10, pp. 1775–1781, Oct. 1993.

[11] J. A. Navarro, J. McSpadden, and K. Chang, "Experimental study of inverted microstrip for integrated antenna applications," in *IEEE Antenna Propagat. Int. Symp. Proc.*, Seattle, WA, 1994, pp. 920–923.

[12] M. Gouker, "Toward standard figures-of-merit for spatial and quasioptical power-combined arrays," *IEEE Trans. Microwave Theory Tech.*, vol. 43, no. 7, pp. 1614–1617, July 1995.

[13] K. D. Stephan and T. Itoh, "Recent efforts on planar components for active quasioptical applications," in *IEEE MTT-S Int. Microwave Symp. Dig.*, 1990, vol. 3, pp. 1205–1208.

[14] K. Chang, *Microwave Solid-State Circuits and Applications.* New York: Wiley, 1994.

[15] P. Bhartia and I. J. Bahl, "Frequency agile microstrip antennas," *Microwave J.*, vol. 25, no. 10, pp. 67–70, Oct. 1982.

[16] E-syn and Libra are registered trademarks of EESof, Inc., Westlake Village, CA.

[17] A. Nesic, S. Jovanovic, I. Radnovic, and D. Nesic, "Integrated uniplanar microwave part of transmitter-receiver with active antennas," *Elecron. Lett.,* vol. 31, no. 21, pp. 1846–1847, Oct. 12, 1995.

Claudio M. Montiel (S'91) was born in San Ramón, Alajuela, Costa Rica, in 1965. He received the B.S. degree in electrical engineering in 1988, from the University of Hawaii at Manoa and the M.S. degree in electrical engineering from Texas A&I University (current name: Texas A&M University, Kingsville), in 1993. Since 1993, he has been at Texas A&M University, where he is pursuing the Ph.D. degree in electrical engineering under the direction of Dr. Kai Chang.

From 1988 to 1991, he was with Western Geophysical Company of America working with seismic data acquisition crews for petroleum exploration in Gabon, Venezuela, and México. His duties included operation, maintenance, and calibration of data recording systems as well as helicopter time and crew management. At Texas A&M University, he has been a Teaching Assistant. His current research interests are in the areas of self-mixing oscillators, active antennas, and conformal antennas.

Mr. Montiel has received The Regents' Fellowship and a fellowship from the U.S. Department of Education.

Lu Fan (M'96), for a photograph and biography, see this issue, p. 2419.

Kai Chang (S'75–M'76–SM'85–F'91), for a photograph and biography, see this issue, p. 2420.